Multi-scale study of the structuration of candle blends with a high content of vegetable fats to replace paraffins: Effect of 12-hydroxystearic acid content

Marie Caroline Agogué, Catherine Loisel, Olivier Gonçalves, Jack Legrand, Sylvaine Saint-jalmes, Abdellah Arhaliass

Received: 28 March 2020 | Revised: 25 March 2022 | Accepted: 11 June 2022

DOI: 10.1002/aocs.12625

ORIGINAL ARTICLE

AOCS WILEY

Multi-scale study of the structuration of candle blends with a high content of vegetable fats to replace paraffins: Effect of 12-hydroxystearic acid content

Marie Caroline Agogué[1] | **Catherine Loisel**[2] | **Olivier Gonçalves**[1] | **Jack Legrand**[1] | **Sylvaine Saint-Jalmes**[3] | **Abdellah Arhaliass**[1]

[1]Nantes University, ONIRIS, CNRS, UMR6144, Saint-Nazaire, France

[2]ONIRIS, Nantes University, CNRS, UMR6144, Nantes, France

[3]Denis et Fils, RN149 Recouvrance, Gétigné, France

Correspondence
Abdellah Arhaliass, Université de Nantes, CNRS, GEPEA, UMR 6144, F-44600 Saint-Nazaire, France.
Email: abdellah.arhaliass@univ-nantes.fr

Funding information
Denis & Fils Company

Abstract

The aim is to replace mineral waxes with vegetable fats as an organogel for candle manufacturing while keeping the same texture. The physico-chemical characteristics of renewable vegetable raw materials differ from those of mineral waxes and consequently the structure of the blends in which they are used is modified. Their properties are measured at different scales using FT-IR analysis, polarized light microscopy, calorimetry and rheology. The addition of 12-hydroxystearic acid (12-HSA) promotes the creation of hydrogen bonds within the rapeseed oil that makes possible its incorporation to form an organogel. The addition of 12-HSA also results in a modification of the crystal microstructure of blends made of 90% vegetable raw materials. Hence, the crystal lattice is denser and the crystal size is reduced compared to blends including mineral waxes. At a macroscopic scale, the physical properties of blends with 12-HSA are modified compared to the reference one, mainly made of mineral waxes. A modification of crystallization and melting temperatures as measured by differential scanning calorimetry as well as the rheological behavior and the hardness assessed by penetrometer are observed. This results in a higher stability against exudation for blends with a high content of 12-HSA. Mineral waxes can thus be substituted in the formulation of candles by renewable materials for the use of organogel, via the incorporation of an organogelator, 12-HSA.

KEYWORDS
crystallization, microstructure, organogel, renewable raw materials

INTRODUCTION

Mineral waxes are by-products of crude oil refining (Wauquier, 1998). They are obtained by distillation in group 1 refineries, which produce base oil with a sulfur content higher than 0.03%. These refineries close day by day and turn to group 3 and 4 refineries that produce base oils with a sulfur content lower than 0.03%; they are more efficient and less polluting. In this way, the availability of mineral waxes is decreasing while needs increase every day. Indeed, mineral waxes are used in many everyday products: for the manufacture of candles, rubber, in pharmaceuticals and cosmetic products, papers and matches (Kraus, 2018). To overcome this lack of supply, alternatives are emerging towards the use of renewable vegetable raw materials. A potential drawback of these vegetable fats is the fact that most of them are liquid or have a low melting point close to room temperature. The structure of the products can thus be impacted and of lower quality leading to migration of oil at their surfaces during storage. In order to provide texture and strength to finished

products, vegetable fats are preferably hydrogenated, partially or totally, or undergo other chemical modifications such as epoxidation or esterification. Wang and Wang's study (Wang & Wang, 2007) shows that the epoxidation of partially hydrogenated soybean oil allows the introduction of new chemical functions, including hydroxyl groups that promote cohesiveness and increase the hardness of the oil. Nowadays, it is well known that vegetable fats like palm stearin (solid fraction mainly made of saturated fatty acids like palmitic and stearic acids) and soy wax present good textural characteristics. These two vegetable fats can be used in candles as a replacement for paraffins (Rezaei et al., 2002). An important characteristic of vegetable fats and waxes is their ability to crystallize. As in all everyday products, food (chocolate, margarine), drug products (suppositories) and cosmetics (lipsticks), crystallization is a phenomenon to be controlled. In particular, the crystallization of chocolate is the subject of numerous studies because it determines the organoleptic and physical characteristics of the finished products (surface crystallization, fat blooming; Loisel et al., 1998). In order to limit this phenomenon of crystallization, the addition of vegetable oils is implemented. However, too much oil causes the system to soften, and the exudation to increase at high temperatures. The use of an organogel could be the solution to incorporate high oil content in a formulation. An organogel is a system composed of an organic liquid and an organogelator, added to a very small percentage (<1%). The organic liquid, here the liquid fat, is solidified at room temperature thanks to the organogelator. Organogels are increasingly used in the food, cosmetics, pharmaceutical and petrochemical industries. Organogels could also be used in candles manufacturing: since, it could limit the incorporation of petrochemical paraffins. They confer many beneficial properties to the products in which they are introduced. In food products (e.g., chocolate, margarine), they allow the substitution of solid fats that may be composed of trans fatty acids, harmful to human health, with polyunsaturated vegetable fats (Hwang et al., 2012; Hwang et al., 2013; Patel, 2015). In the field of cosmetics (Iwanaga et al., 2010; Kirilov et al., 2015), gels are mainly used for their ability to vectorize molecules of interest through the skin to the target organs. In addition, these gels are transparent and very stable because of their structure. Organogelators form a three-dimensional network that traps the liquid fraction, the vegetable fat that is liquid at room temperature. Various molecules are considered to be organogelators: vegetable waxes (like Candelilla wax, Carnauba wax, Beeswax; Hwang et al., 2012), fully hydrogenated vegetable fats (hydrogenated castor oil) and fatty alcohols (12-hydroxystearic acid, 12-HSA). 12-HSA is a hydroxylated fatty acid obtained from the hydrogenation of ricinoleic acid, the main fatty acid of castor oil (more than 90%). 12-HSA is already the subject of numerous studies for which it is mixed with a single fat, a vegetable oil. Co and Marangoni (2013) studied the impact of shear and cooling rate on the microstructure of 12-HSA in canola oil: too high shearing and too fast cooling of the system lead to gel destructuring, thus causing the oil to be released from the system. They also demonstrated the mechanism of 12-HSA imparting structure to canola oil as unique fibrillar crystal habit. Rogers and Marangoni (2008, 2009) highlighted the difference in crystallization and in particular the nucleation of 12-HSA in different solvents (canola oil, mineral oil, triolein, methyl oleate and glycerol) at different cooling rates. The nature of the solvent affects the nucleation rate, crystal size, crystal distribution and degree of branching. However, the impact of 12-HSA in more complex blends, that means a blend of several vegetable fats in a combination with an organogelator, has not yet been studied.

The objective of this article was to increase the content of renewable raw materials as a substitute of petrochemical paraffins for making candles. This was performed by replacing mineral waxes to a large extent by an organogel made of 12-HSA and rapeseed oil in blends and by increasing the content of rapeseed wax. In this way, the part of renewable material including 12-HSA increased from 40.5% in the reference blend to 90% in the modified blends. The impact of 12-HSA, at different concentrations on the structure of candle blends made of high content of renewable raw materials, in particular on their microstructure was investigated. For this purpose, the structure was analyzed at three scales: at molecular scale, using the infrared spectra, at microscopic scale, by polarized light microscopy to characterize the size distribution of the crystals, and at macroscopic scale by measuring rheological behavior and hardness of these blends. The phase transition of blends was analyzed by differential scanning calorimetry (DSC).

MATERIALS AND METHODS

Raw materials

A mineral wax with a low crystallization point (47–52°C) was purchased from Sasol Wax GmbH (Hamburg, Germany). The rapeseed wax, having a high melting point (65–70°C) and the rapeseed oil, liquid at room temperature, were both obtained from Cargill (Schiphol, The Netherlands). 12-HSA (melting point of around 75°C) was purchased from Castor International (Deume, The Netherlands). The blend made of 12-HSA and rapeseed oil is called organogel.

Raw materials pure and mixed in the different blends were analyzed. First of all, the chemical compositions of these raw materials were determined by gas chromatography with an Agilent 7820A, TR-FAME

TABLE 1 Formulation of the reference and modified blends (% wt/wt)

		Modified blends			
	Reference Blend	**Mod1.4**	**Mod3.5**	**Mod4.9**	**Mod7**
Mineral wax	59.5	10.0	10.0	10.0	10.0
Rapeseed wax	10.5	20.0	20.0	20.0	20.0
Rapeseed oil	30.0	68.6	66.5	65.1	63.0
12-HSA	-	1.4	3.5	4.9	7.0

column 260M142P (0.25 mm i.d., 0.25 μm thickness, 30 m length; ThermoFisher Scientific, France). Thus, the results of this analysis showed that rapeseed wax contains mainly stearic acid (91.4%), while rapeseed oil contains mostly unsaturated fatty acids (67.4% of oleic acid and 24.1% of linoleic acid). 12-HSA is made of stearic (84.8%) and palmitic (11.5%) acids. Mineral wax contains 92.3% of *n*-alkanes, mostly medium chains (23–28), and 7.7% of iso-alkanes.

Preparation of samples

Two types of mixtures were studied: a reference blend and four modified blends. The composition of the five blends is presented in Table 1. The reference blend is composed of 40.5% vegetable fats and 59.5% mineral wax. The modified blends contain 90% of renewable raw materials. They are composed of 70% organogel, 20% rapeseed wax and 10% mineral wax. The organogel consists of rapeseed oil and 12-HSA. Different contents of 12-HSA were tested within the organogel: 2%, 5%, 7% and 10% wt/wt. The modified blends are named Mod1.4, Mod3.5, Mod4.9 and Mod7 according to their 12-HSA content. No blank sample without 12-HSA was studied: as the reference blend was commercialized, the substitution of petrochemical paraffins by an organogel (in the modified blends) is compared to this reference blend. The organogel is prepared by adding 12-HSA to rapeseed oil in a stainless jug and heated to 85°C to ensure the melting of 12-HSA. All the blends were prepared in triplicate by mixing and heating the raw materials until 85°C in a stainless jug. The samples were then cooled at room temperature except when cooling is controlled for thermal analysis (calorimetry, rheology) and crystal size analysis (microscopy). All the modified blends, as the reference blend, were opaque, independently of 12-HSA content. All testing were conducted on these triplicate blends.

Chemical composition of raw materials and blends by FT-IR analysis

The chemical analysis of raw materials and blends was completed by the analysis of the main chemical functions by a Bruker tensor 27 FTIR spectrometer (Bruker Optics, Germany) equipped with an attenuated total reflection mode (ATR) platinum module, with a deuterated triglycine sulphate detector RT-DLaTGS. Infrared spectra were recorded on the single reflexion diamond crystal of the ATR accessory loaded with one drop of liquid materials or a few milligrams of solid raw materials. The spectrometer was set up with the following parameters: the spectral resolution was fixed to 4 cm^{-1}, the number of scans to 16, the selected spectra ranged between 4000 and 400 cm^{-1}. Background spectra were collected using the same instrument settings and were performed against air. Spectra were analyzed using the OpusLab v7.0.122 software. Spectra were recorded for three replicates per sample.

Fat crystal structure by microscopy

Observation of crystalline microstructure by polarized light microscopy

The microstructure of raw materials and blends was observed using polarized light microscopy (Leica Microsystems, DM R, Germany). Crystallization of samples was directly performed on microscope slide. First of all, crystal memory of each sample was erased by melting to 80°C. Microscope slide was also heated at 80°C. A small amount of sample, around 1 μl, was put on the slide and covered by a cover slip. The prepared slides are then cooled at room temperature during 1 h. Three images per sample were acquired with a CCD camera and were treated with Visilog software.

Crystals size analysis of blends

The crystal size distribution was determined by the ImageJ software, according to the following steps: thresholding (white crystals on a darkfield), then edge cutting and finally individualization of the crystals. Each crystal was characterized by its maximal Feret diameter, which defines the distance between two tangents including the crystal at a given orientation (0°, 45° or 90°). Fifteen classes of maximal Feret diameter were determined according to a geometrical progression of reason **R**, using the following formula:

$$R = \left(\frac{\text{largest maximal Feret diameter}}{\text{smallest maximal Feret diameter}}\right)^{1/N},$$
where $\boldsymbol{N}$ is the number of classes $(N = 15)$

The calculated reason was thus equal to 1.30. The number size distribution was plotted to determine the median diameter $\boldsymbol{d_{50}}$ and the $\boldsymbol{d_{90}}$. This analysis was carried out on three images of a same blend corresponding to about 900 crystals per image.

Melting and crystallization properties by differential scanning calorimetry

A wax sample of 7.0–10.0 mg was placed in an aluminum cup. A calibration was made with indium as the standard, on the calorimeter Q100 (TA Instruments, New Castle, DE, USA). The temperature program was: 3 min at 20°C followed by an increase to 80°C at 5°C/min with a 3 min hold at 80°C to ensure complete melting. Then the sample was cooled to −10°C at 5°C/min and held at this temperature during 20 min to achieve complete crystallization. Finally, the sample was heated to 80°C at 5°C/min and held at this temperature for 3 min. The onset temperatures, peak temperatures and enthalpies of crystallization and melting were determined from the cooling and second heating steps respectively (Universal V4.5A TA Instruments software).

The solid fat content (SFC) of each sample was also determined by using the crystallization curve during the cooling from 80°C to −10°C at 5°C/min rate. The SFC was plotted as a function of the temperature by integrating the crystallization curve for each temperature T, thanks to the following equation (Raemy & Lambelet, 1991; Universal V4.5A TA Instruments software):

$$\mathrm{SFC(T)} = \frac{\int_{T_0}^{T} \mathrm{H(T)dT}}{\int_{T}^{T_1} \mathrm{H(T)dT}}$$

where $\mathbf{T_0}$ is the onset temperature of crystallization (°C), $\mathbf{T_1}$ is the end temperature of crystallization (°C) and **H(T)** is the enthalpy (J g^{-1}).

Each sample was measured three times.

Mechanical properties of blends by rheology

Determination of viscosity under flow

The viscosity of blends was determined on cooling on the Physica MCR500 rheometer (Anton PAAR, Courtaboeuf, France) using two coaxial cylinders and 20 ml sample (CC27, 26.66 and 28.92 mm diameters). With this geometry, no wall slip could be identified. The following protocol was applied: first, a stabilization for 60 s at 70°C, at 1 s^{-1} and then a cooling from 70 to 30°C at 5°C/min at 20 s^{-1}. Three measurements per sample were performed.

Determination of the viscoelastic properties under oscillation

During this analysis, the elastic (G') and viscous (G'') moduli of the blends were determined using the Physica MCR500 rheometer (Anton PAAR, Courtaboeuf, France) with two coaxial cylinders (CC27, 26.66 and 28.92 mm diameters). With this geometry, no wall slip could be identified. Measurements were made at constant frequency ($f = 1$ Hz) and with an imposed strain of 0.1% in the linear domain. A volume of 20 ml of sample was placed in the fixed cylinder, heated at 70°C for 3 min, then cooled to 30°C at 5°C/min and stabilized at 30°C for 3 min. Three measurements were made per sample.

Hardness of blends by penetrometry

The hardness of the five blends was measured using a Petrotest® PNR10 penetrometer (Villeneuve La Garenne, France). For this purpose, the blends were melted and poured into metal buckets at 70°C. They were then cooled to room temperature and maintained at that temperature for 1 hour. The buckets were finally placed in a water bath at the considered temperature (25 or 40°C) for 1 h. Penetrability measurements were made at these two temperatures and expressed as the penetration depth of the needle into the studied blend during 5 s. Five measurements were performed by blend.

Statistical analysis

The statistical analyses were performed using XLSTAT statistical analysis software (Addinsoft, Bordeaux, France). Analysis of variance (ANOVA) followed by a Fisher test (LSD) to compare means were performed on experimental data. There were three replicates for each measurement for each blend, except for the hardness test where were five replicates. The level of significance used for this test was 5%.

RESULTS AND DISCUSSION

Molecular structure: Chemical composition

The infrared spectra of the raw materials alone and the reference and modified blends are given in

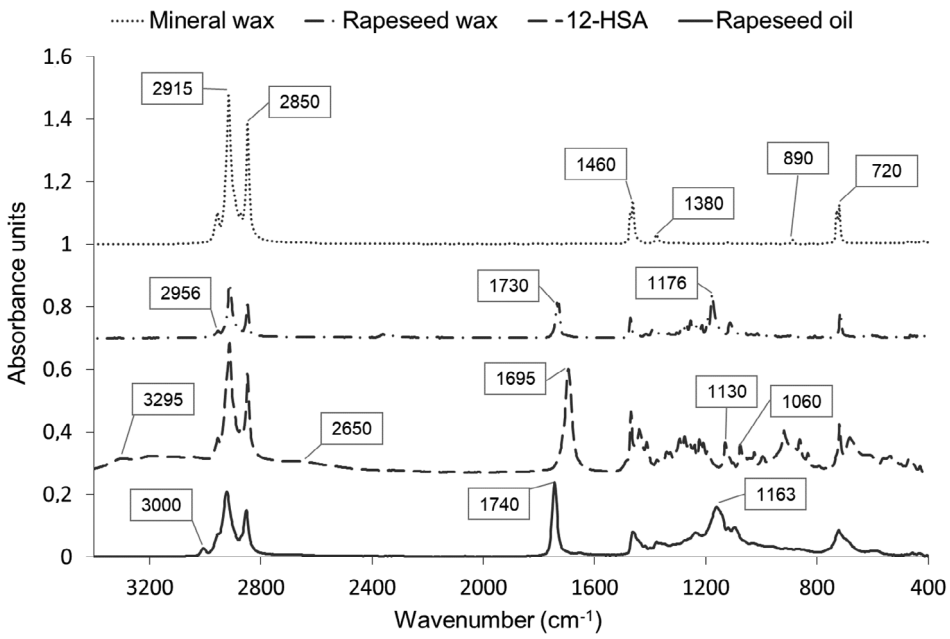

FIGURE 1 Infrared spectra of raw materials

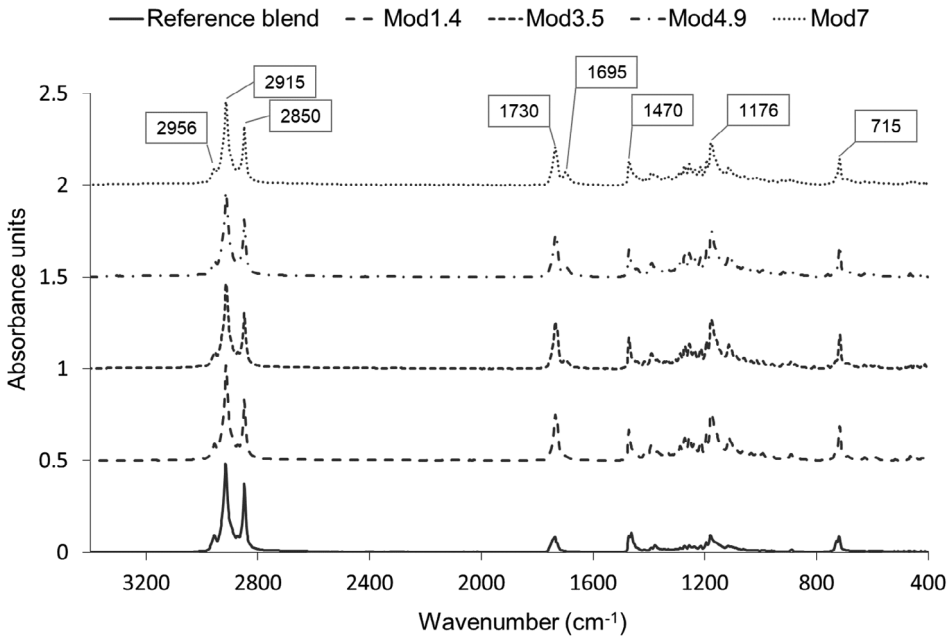

FIGURE 2 Infrared spectra of reference and modified blends

Figures 1 and 2, respectively. The correspondence of the peaks obtained with the different chemical bonds is determined using correlation tables (Merck, n.d.; INSA Rouen, 2020; Canesi, 2020). The percentage of each chemical groups was not calculated, only the nature of these chemical groups and the potential interactions between them were studied. The spectra of vegetable materials (rapeseed wax and rapeseed oil), shown in Figure 1, highlight the main chemical functions characterizing these types of materials: the C—C bonds of alkanes (2850, 2915 and 1460 cm^{-1}), the C—O bond of the typical ester function of triglycerides (1176 cm^{-1}), the C═O bond of carboxylic acids at 1380 and 1470 cm^{-1} and unsaturations represented by peaks at 720 cm^{-1}. 12-HSA spectrum has the same chemical functions as the vegetable fats with two particularities: an absorbance range between 2650 and 3295 cm^{-1} and two peaks at 1060 and 1130 cm^{-1} appear on the spectrum. These peaks correspond respectively to the O—H bond of the alcohol group and the C—O bond of a secondary alcohol. This clearly shows the substitution of a hydrogen by a hydroxyl group on the aliphatic chain of 12-HSA. The spectrum of mineral wax is less complex than those of vegetable fats. Indeed, only the C—H bonds of alkanes appear (at 720, 1380, 1460, 2850 and 2956 cm^{-1}).

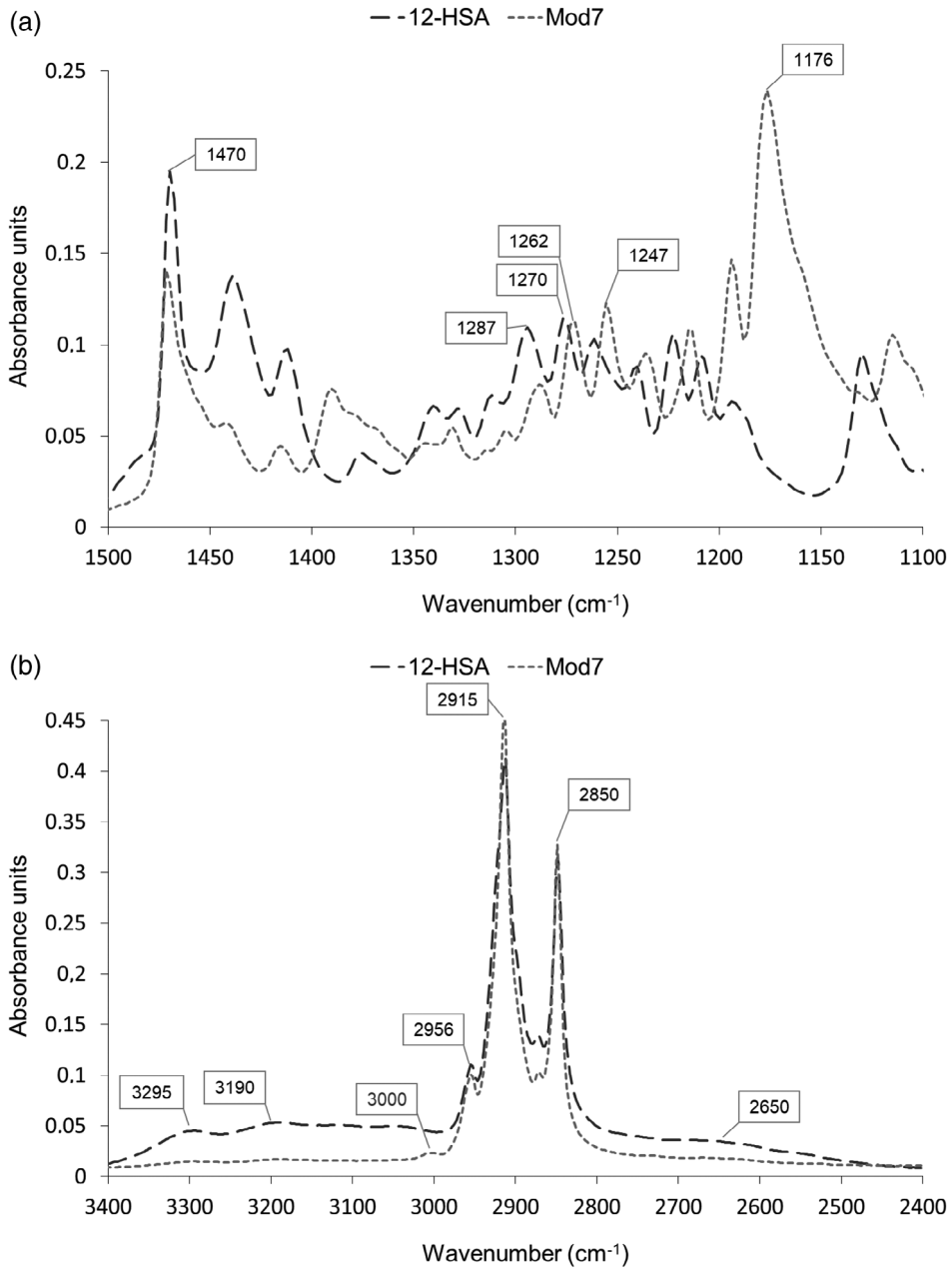

FIGURE 3 Infrared spectra of Mod7 compared to infrared spectra of 12-HSA focusing on hydroxyl regions (a: Between 1500 and 1100 cm^{-1}, and b: Between 3400 and 2400 cm^{-1})

A low intensity peak is also present at 890 cm^{-1}, suggesting the presence of a C═C double bond, highlighting the presence of an oily part in the mineral wax, because of its partial refining. Concerning the spectra of the four blends (Figure 2), the appearance of these spectra clearly shows the different peaks obtained for the raw materials described before. There are therefore no chemical transformations, such as the formation of covalent bonds between raw materials for neither the reference nor the modified blends, that could be detected upon the prism of FT-IR analysis. By adding 12-HSA (Figure 2), a peak appears at 1695 cm^{-1}. By observing more precisely the peaks at 1730 and 1695 cm^{-1}, a carboxylic acid dimerization is observed at 1695 cm^{-1} corresponding to a gelation of the rapeseed oil by 12-HSA. The intensity of this peak is all the more important when the 12-HSA content is high. On the contrary, the higher the 12-HSA content, the lower the intensity of the peak at 1730 cm^{-1}. By comparing the spectrograms of 12-HSA and Mod7 (Figure 3a), a shift from specific peaks of O—H bonds to lower frequencies (from 1287 to 1262 cm^{-1} and from 1270 to 1247 cm^{-1}) is observed. In addition (Figure 3b), the peak corresponding to the O-H bond stretch is very wide (between 2400 and 3400 cm^{-1}) and centered on the peak of the C-H stretching region showing strong hydrogen bonds between the carboxylic functions of vegetable raw materials and the hydroxyl group of 12-HSA. Thus, hydrogen bonds are created both between 12-HSA molecules and

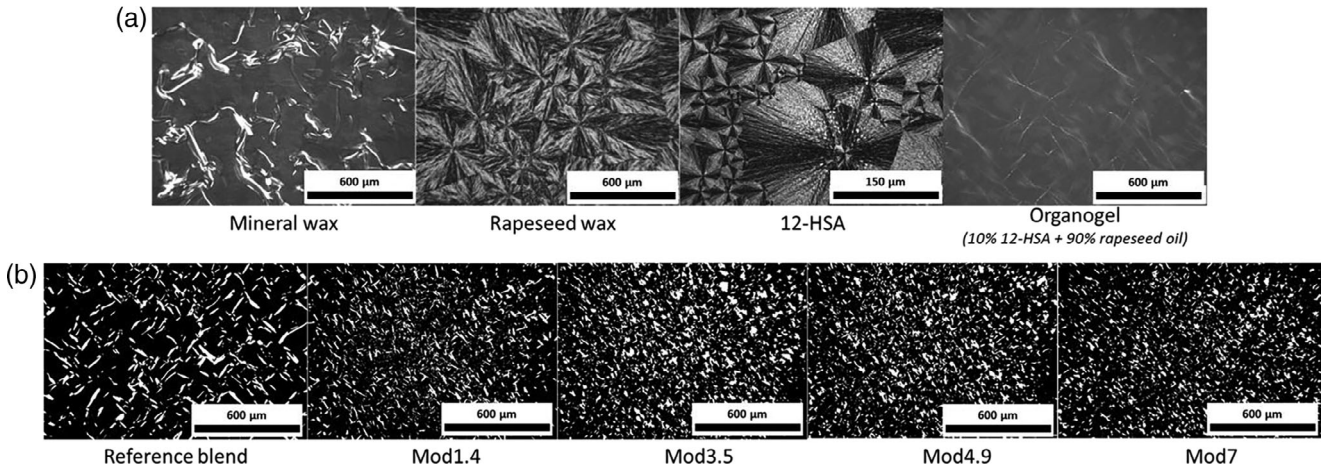

FIGURE 4 Polarized light microscopic images of raw materials (a) and blends after thresholding by ImageJ (b) at room temperature

between 12-HSA and rapeseed oil. These observations are supported by those made by Wu et al. (2013).

Microstructure: Crystals morphology by polarized light microscopy

In order to compare the microcrystalline structure of blends with and without 12-HSA, polarized light microscopy images were performed (Figure 4). First of all, the microcrystalline structures of raw materials used in the different blends such as mineral wax, rapeseed wax, 12-HSA and the organogel (made of 10% wt/wt of 12-HSA and 90% wt/wt of rapeseed oil) were analyzed. The structure of mineral wax is completely different from the one of vegetable raw materials. The crystals of the mineral wax present rod-like forms while rapeseed wax and 12-HSA present a spherulitic microstructure, like Maltese crosses. The organogel presents a fibrillar microstructure exhibiting segmented birefringence. This result is consistent with Co and Marangoni (2013) when studying the crystallization of an organogel formed by 12-HSA in canola oil. The reference blend (Figure 4b) has a particular crystalline microstructure: the crystals present a rod-like form and a homogeneous and organized crystal lattice. The addition of 12-HSA significantly alters the microstructure of blends. The crystals of modified blends are smaller, more numerous and do not have exactly the same shape as those of the reference. The characteristic diameters of the blends are determined thanks to cumulative frequencies (Figure 5): d_{90} of the reference blend is equal to 25 µm against 9.0, 8.9, 10.1 and 7.2 µm for Mod1.4, Mod3.5, Mod4.9 and Mod7, respectively. Addition of 12-HSA seems to have a beneficial effect by limiting crystallization. The median diameters d_{50} of the modified blends are rather similar whatever the concentration of 12-HSA: Mod1.4 and Mod7 have a d_{50} of 1.8 and 1.9 µm respectively, while Mod3.5 and Mod4.9 blends have a d_{50} of 2.5 and 3.1 µm respectively. The reference blend differs from the modified blends with a median diameter of 5.1 µm. In the modified blends, the crystals are particularly small, more numerous and thus form a denser lattice by filling more of the free space corresponding to the liquid fraction. The ability to trap the liquid fraction might therefore increase, resulting in a decrease in the exudation of the blends. 12-HSA is therefore considered as a crystallization initiator.

One of the benefits of using organogels made of vegetable oil and 12-HSA instead of vegetable waxes, such as Candelilla, Carnauba, rice bran and cane sugar waxes or animal waxes such as beeswax, is their specific crystalline microstructure. Indeed, the microstructure of organogels made of 12-HSA and rapeseed oil, as shown by the polarized light microscope images (Figure 4a), is much finer than the ones of vegetable waxes: the crystals are finer and more elongated (Blake et al., 2014; Jana, 2016; Patel, 2015). It has already been shown by Co and Marangoni (2013) that 12-HSA crystallizes in one axis, the fiber axis, and form fiber-like crystals. In this structure, non-covalent cross-links (like hydrogen bonding, determined by FT-IR) are made forming the so-called self-assembled fibrillar network (SAFiN). The crystallization of mixtures in which 12-HSA is incorporated is thus limited; the homogeneity of the blends is therefore improved. In addition, by increasing the density of the crystalline network of the blends in the presence of 12-HSA, the exudation of the blends is reduced by trapping the rapeseed oil via capillary forces. This observation could be verified by placing the four blends containing the organogel in an oven preheated at 40°C: the higher the 12-HSA content, the less the exudation (results not shown).

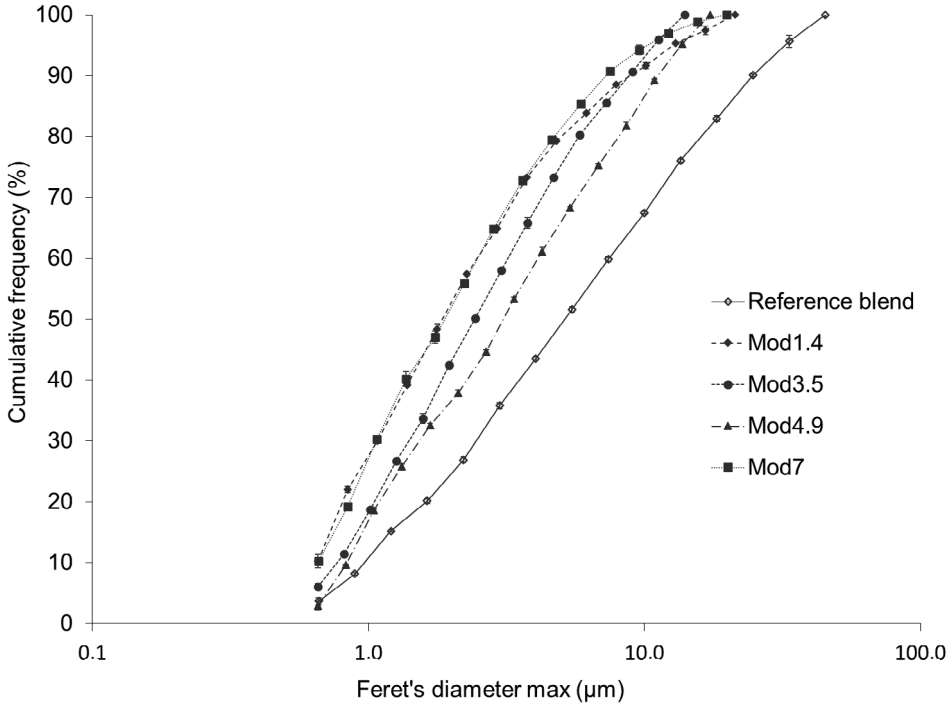

FIGURE 5 Cumulative frequencies in number (%) of the fat crystals size in reference and modified blends (mean standard deviation = 0.4%)

Phase transition: Melting and crystallization profiles by differential scanning calorimetry

The crystallization and melting profiles of the raw materials and the blends are presented in Figure 6. The enthalpies, the onset and end temperatures and the peaks temperatures of crystallization and melting are presented in Table 2.

The thermal profiles of the isolated raw materials (Figure 6a) and blends (Figure 6b,c) are compared. Rapeseed oil is not represented because of its liquid state at positive temperatures. For the reference blend in Figure 6b, the first crystallization peak, at 45.1°C, could correspond to the crystallization peak of rapeseed wax (Figure 6a). The second peak of crystallization, at 33.9°C, could correspond to the major peaks of the mineral and rapeseed waxes. It should be emphasized the fact that the mineral wax because of its very broad composition of *n*-alkanes, mostly medium chains from 23 to 28 (this was determined by gas chromatography) exhibits a large range of melting temperatures. The same approach can be used for the modified blends and particularly for Mod7: the crystallization peak of Mod7 at 51.4°C could correspond to the 12-HSA peak, and the major peaks of Mod7 and Mod 4.9 at 42°C would correspond to the crystallization peak of the rapeseed wax at 47.0°C. A clear shift towards peak temperatures is observed between the profile of the isolated raw materials and the blends.

The impact of adding 12-HSA as an organogel to blends is shown in Table 2. The content of 12-HSA in final blends affects considerably the crystallization and melting profiles: number and temperature of peaks, onset temperatures and enthalpies are modified. The higher the 12-HSA content, the higher the onset temperature of crystallization. Nevertheless, only Mod4.9 and Mod7 blends have higher onset temperatures of crystallization compared to the reference blend. The temperature ranges between the onset and the end of crystallization are less wide for the modified blends than for the reference blend, and it depends on the 12-HSA content in the modified blends: the higher the 12-HSA content, the lower the temperature range of peaks (Table 2). The crystallization and melting enthalpies are halved for the modified blends. In the melting profiles of the modified blends (Figure 6c) and especially Mod4.9 and Mod7, a crystallization is observed during melting (around 46°C), which did not happen for the reference blend. This can be because of a rearrangement of molecules in the crystalline lattice. These differences of enthalpies and ranges of temperatures between the reference and the blend could have an impact on the melting behavior, thus causing difficulty in melting. The crystallization temperature of the different blends was determined (Figure 6b): Mod1.4 and Mod3.5 have a lower crystallization temperature than the reference blend. On the contrary, Mod4.9 and Mod7 have a higher crystallization temperature than the reference blend. This parameter is important during the manufacture of final products: it allows to determine the pouring temperature of the blends in containers. With regard to the melting profiles of the reference and modified blends (Figure 6c), the liquid fat content is reduced by the addition of 12-HSA and in particular at

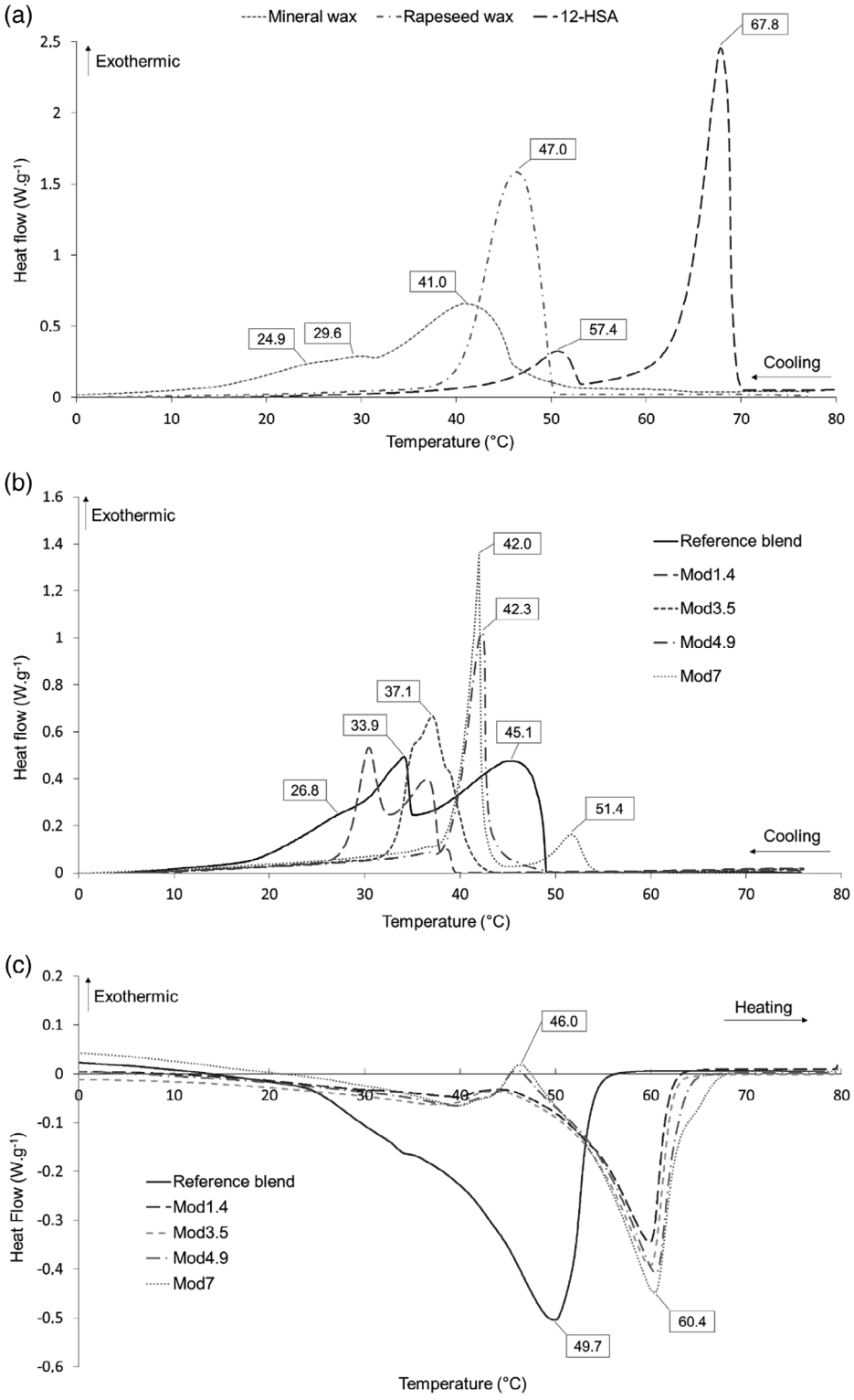

FIGURE 6 Differential scanning calorimetry recordings of crystallization of raw materials (a) and crystallization (b) and melting (c) of blends at a cooling rate of 5°C/min

room temperature and at higher temperatures around 35–40°C.

The solid fat content (SFC) profiles of the raw materials and the five blends are determined by integrating the crystallization curve obtained by DSC and are shown in Figure 7. Mineral and vegetable waxes (Figure 7a) have solid fat content decreasing between 50 and 60°C. 12-HSA melts at much higher temperatures (Figure 6a): it is totally liquid at 70°C. The SFC profiles (Figure 7b) of the four modified blends differ: the higher the content of 12-HSA, the higher the melting point. Moreover, a difference in solid fat content is observed between the reference and the modified blends between 25 and 45°C. The SFC of the modified

TABLE 2 Enthalpy, onset temperatures, peak and end temperatures of crystallization and melting of raw materials and blends depending on 12-HSA content obtained by DSC (at a cooling rate of 5°C/min)

	Crystallization						Melting			
	Measured total enthalpy ($J.g^{-1}$)	Onset temperature (°C)	Peak temperatures (°C)			End temperature (°C)	Measured total enthalpy ($J.g^{-1}$)	Onset temperature (°C)	Peak temperature (°C)	End temperature (°C)
			1st peak	2nd peak	3rd peak					
Mineral wax	140.9 ± 6.9^{b}	60.0 ± 0.3^{b}	41.0 ± 0.1^{c}	29.6 ± 0.8^{b}	24.9 ± 0.6	13.9 ± 0.2^{c}	138.1 ± 5.4^{b}	20.0 ± 0.1^{c}	45.8 ± 0.1^{c}	71.8 ± 0.1^{c}
Rapeseed wax	131.4 ± 0.9^{c}	50.1 ± 0.1^{c}	47.0 ± 0.4^{b}			38.6 ± 0.1^{b}	156.4 ± 10.3^{a}	50.1 ± 0.1^{a}	69.6 ± 0.1^{b}	76.2 ± 0.1^{b}
12-HSA	153.2 ± 0.4^{a}	69.1 ± 0.1^{a}	67.8 ± 0.2^{a}	57.4 ± 0.3^{a}		42.5 ± 0.1^{a}	151.8 ± 0.7^{a}	44.8 ± 0.1^{b}	77.9 ± 0.4^{a}	84.0 ± 0.1^{a}
Mod1.4	48.9 ± 0.1^{E}	39.5 ± 0.1^{E}	38.7 ± 0.1^{C}	36.6 ± 0.3^{B}	30.4 ± 0.7^{C}	26.1 ± 0.3^{D}	47.1 ± 0.1^{D}	11.3 ± 0.1^{D}	59.9 ± 0.3^{B}	63.8 ± 0.1^{B}
Mod3.5	54.2 ± 0.1^{C}	42.2 ± 0.1^{D}	39.0 ± 0.2^{C}	37.1 ± 0.3^{B}	35.1 ± 0.1^{B}	31.9 ± 0.1^{C}	52.2 ± 0.1^{C}	9.0 ± 0.1^{E}	59.8 ± 0.2^{B}	63.8 ± 0.2^{B}
Mod4.9	53.4 ± 0.1^{D}	50.0 ± 0.1^{B}		42.3 ± 0.1^{A}	36.9 ± 0.3^{A}	35.9 ± 0.1^{A}	54.1 ± 0.1^{B}	21.4 ± 0.1^{C}	60.5 ± 0.5^{A}	65.9 ± 0.1^{C}
Mod7	62.4 ± 0.1^{B}	53.8 ± 0.2^{A}	51.4 ± 0.3^{A}	42.0 ± 0.1^{A}	37.4 ± 0.1^{A}	34.9 ± 0.1^{B}	54.2 ± 0.1^{B}	22.9 ± 0.2^{B}	60.4 ± 0.1^{A}	69.1 ± 0.1^{D}
Reference blend	116.6 ± 3.2^{A}	48.9 ± 0.1^{C}	45.1 ± 0.4^{B}	33.9 ± 0.6^{C}	26.8 ± 0.3^{D}	16.9 ± 0.2^{E}	114.9 ± 3.3^{A}	25.0 ± 0.1^{A}	49.7 ± 0.2^{C}	57.2 ± 0.1^{A}

Note: For each parameter, means with the same letter are not significantly different (ANOVA, $p \leq 0.05$, Fisher test). Lower case letters are used for the raw materials and upper-case letters are used for the blends.

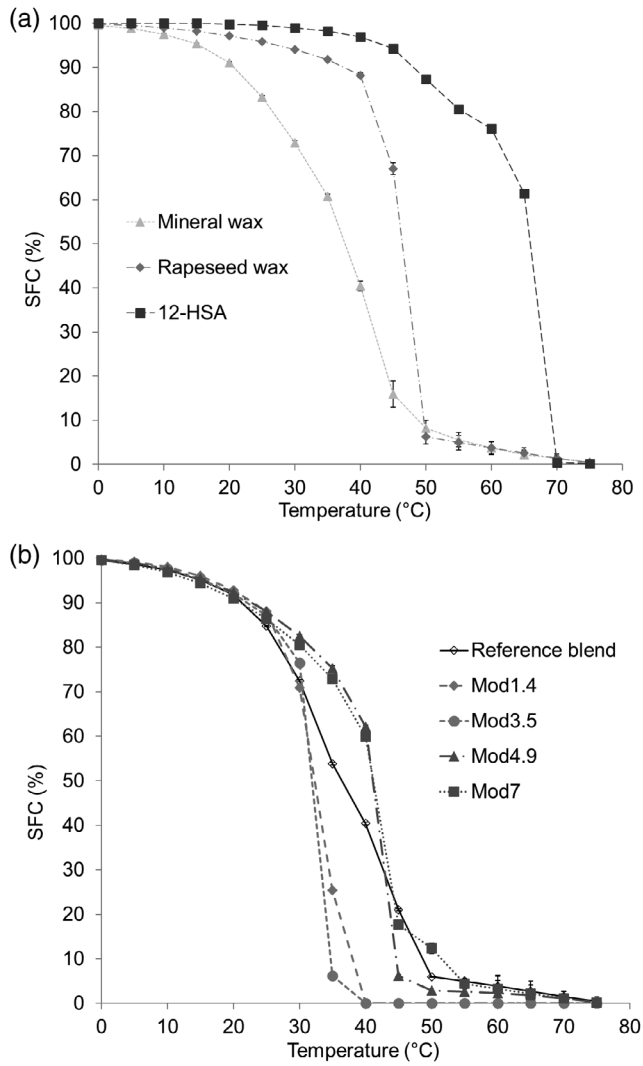

FIGURE 7 Solid fat content (SFC) profiles of raw materials (a) and blends (b) (mean standard deviation = 0.6%)

blends (Mod4.9 and Mod7) is higher than that of the reference blend limiting exudation at high temperatures. The thermal stability of these modified blends is therefore improved. This is not the case for blends having a 12-HSA content less than 4.9%.

Phase transition: Mechanical properties measured by rheology

All the studied blends in the liquid state behave like Newtonian fluids; the viscosity is independent of the shear rate. To monitor the evolution of viscosity during crystallization, a shear rate of 20 s^{-1} was applied. Figure 8 shows the variation of viscosity of the five blends during cooling (from 70 to 20°C at 5°C/min). The modified blends have a higher viscosity than the reference blend at high temperatures, when they are completely melted. The modified blends are therefore more viscous at temperatures higher than 60°C: more

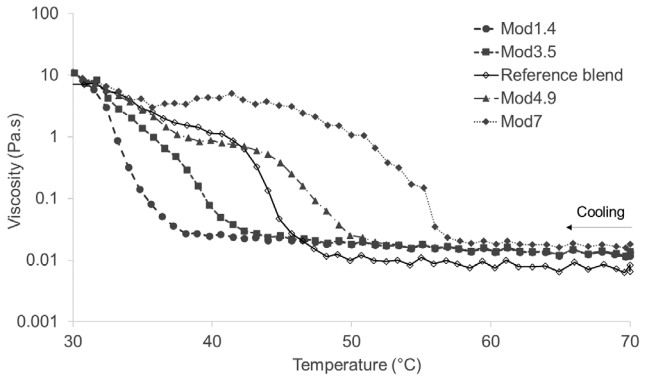

FIGURE 8 Evolution of the viscosity of the reference and modified blends during cooling at 5°C/min under a shear rate of 20 s^{-1}

than 0.01 Pa.s for the modified blends against 0.008 Pa.s for the reference blend. The 12-HSA content influences significantly the viscosity. Indeed, at a content of 7%, the viscosity increases: 0.018 Pa.s for Mod7 against 0.015 Pa.s for Mod1.4, Mod3.5 and Mod4.9.

The crystallization of the blends induces an increase in viscosity; the temperatures at which crystallization begins can thus be determined. The reference blend begins to crystallize at 47°C. This temperature is modified by adding 12-HSA. The higher the 12-HSA content, the higher the temperature at which crystallization begins. For contents of 1.4% (Mod1.4) and 3.5% (Mod3.5), the crystallization temperature is 36.4 and 41.6°C, respectively; they are lower than that of the reference. On the contrary, 12-HSA contents higher or equal to 4.9% lead to higher crystallization temperatures compared to the reference (50.6°C for Mod4.9 and 57.7°C for Mod7). The same observations can be made by observing the viscoelastic moduli (Figure 9). The crystallization temperature corresponds to the crossing of the curves of the two moduli: 45°C for the reference and 33, 40, 48 and 52°C for the modified blends Mod1.4, Mod3.5, Mod4.9 and Mod7 respectively. Above these temperatures, the blends have a viscous behavior while below these temperatures, they behave like viscoelastic systems. Differences in crystallization temperatures are observed with the DSC (39.5, 42.2, 50.0 and 53.8°C for Mod1.4, Mod3.5, Mod4.9 and Mod7 respectively) although they remain within the same orders of magnitude. This could be a result of cooling rates that are not the same and to the sample size that is more important for rheological measurements and affects the temperature of the considered sample.

As shown with polarized light microscope images and the crystals size analysis, modified blends have a denser crystalline lattice and are therefore more compact and better structured. More connexions between crystals are thus created, increasing the strength of this network and thus viscosity. However, only Mod4.9 and Mod7 exhibit onset temperatures of crystallization higher

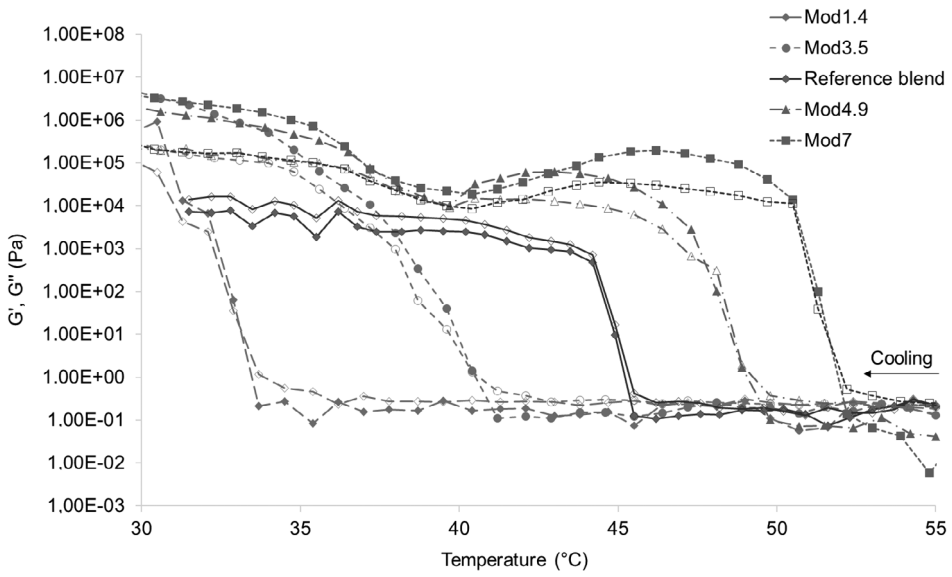

FIGURE 9 Viscoelastic moduli *G'* (close symbols) and *G''* (open symbols) of the reference and modified blends under cooling at a cooling rate of 5°C/min ($f = 1$ Hz, deformation of 0.1%)

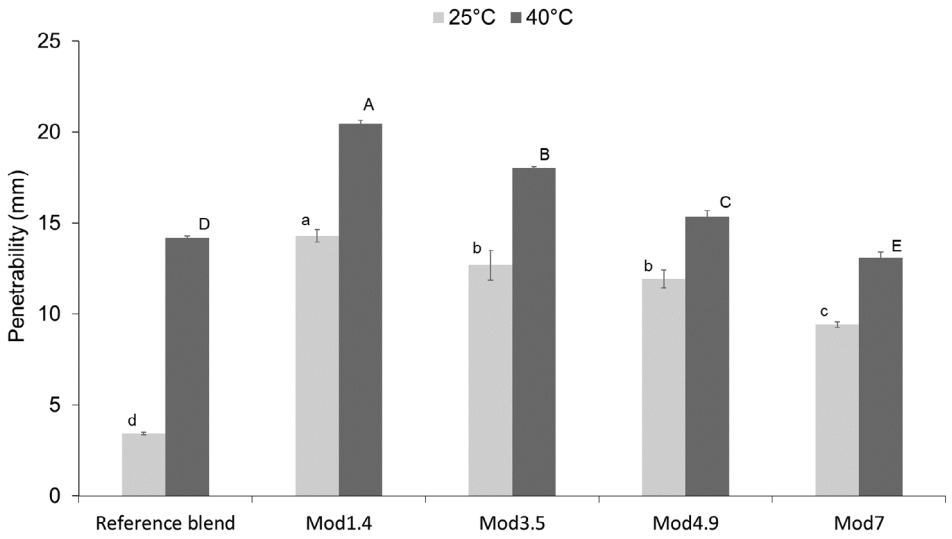

FIGURE 10 Hardness of the reference and modified blends measured by penetrometry at 25 and 40°C (for each temperature, means with the same letter are not significantly different [ANOVA, $p \leq 0.05$, Fisher test]. Lower case letters are used for 25°C and upper-case letters are used for 40°C)

than those of the reference blend (50°C for Mod4.9 and 53.8°C for Mod7 compared to 49.0°C for the reference). The formation of the crystal lattice of these two modified blends thus appears at higher temperatures leading to an increase in the viscosity. It is completely different for Mod1.4 and Mod3.5, their onset temperatures of crystallization are lower than that of the reference (39.5°C for Mod1.4 and 42.2°C for Mod3.5 compared to 49.0°C for the reference). Thus, the crystal lattice may be less structured than for higher 12-HSA contents.

Macrostructure: Hardness measured by penetration measurement

The results obtained from penetration measurements at 25 and 40°C for the reference and modified blends are shown in Figure 10. These measurements calculate the distance traveled by the needle in the blend during 5 s; the higher the penetrability values, the softer the blend. At 25°C, the penetrabilities of the modified blends are more important than the reference. This results to the high rapeseed oil content and the decrease in the mineral wax content. For high temperatures (40°C), the same trend is observed for two lower concentrations (1.4% and 3.5% HSA). However, the Mod7 is harder than the reference blend (13.10 ± 0.30 mm for Mod7 against 14.16 ± 0.14 mm for the reference). The hardness of Mod4.9 is close to the hardness of the reference. The hardness of the blends significantly depends on the microstructure: as shown by microscopy analysis, the crystals of the reference blend are larger than those of the modified blends. This induces a higher hardness at 25°C. A correlation between these results and those obtained by DSC can be made: the SFC of Mod4.9 and Mod7 is more important than the SFC of the reference at high temperatures. In addition, as can be seen on melting

profiles (Figure 6c), the SFC of these same modified blends is higher than that of the reference blend around 40°C. The liquid fraction in these blends is therefore lower, which justifies a higher hardness. In addition, at any temperature, the higher the 12-HSA content in the modified blends, the higher the hardness. 12-HSA provides hardness because of its high melting temperature. As shown by IR spectra, the hydrogen bonds created between 12-HSA molecules and rapeseed oil are all the more important when the 12-HSA content is high. Interactions between molecules are therefore more important, promoting a harder blend.

CONCLUSION

The addition of 12-HSA as organogel in complex blends of vegetable fats and mineral wax modifies the structure at all scales. From a molecular point of view, stated by FT-IR measurements, many weak bonds such as hydrogen bonds are created between 12-HSA molecules and between 12-HSA hydroxyl groups and triglyceride hydroxyl groups from vegetable wax. The higher the 12-HSA content, the higher the extent of the hydrogen bonds. This has an impact on structure at the microscopic scale and on the physical properties at macroscopic scales. Indeed, the crystalline microstructure of modified blends is denser and the crystals finer and smaller. This modification of the crystal lattice leads to a change in the behavior of these blends under temperature fluctuations. The onset temperatures of crystallization are thus impacted, as shown by DSC and rheology. The extent of this modification depends on the 12-HSA content: contents higher or equal to 4.9% lead to higher onset temperatures of crystallization. Blends containing 12-HSA are more viscous than the reference one. All these observations highlight the benefits of adding 12-HSA in complex blends: increasing the rate of renewable materials as a substitute for petroleum paraffins, limiting the crystallization of raw materials thanks to the modification of the crystal lattice by acting like a crystallization initiator and thus improving the macroscopic aspect of finished products. Blends with a 12-HSA content higher or equal to 4.9% are thus harder at high temperatures limiting the potential exudation by releasing the oily part at the surface under the effect of temperature increasing. Thus, thanks to the different results obtained in this research, the best formulation would be the one having the higher content of 12-HSA in the organogel, Mod7, to produce candles. The tendency evolving towards natural, biosourced products, the replacement of mineral raw materials by vegetable raw materials could be an effective alternative. Thus, the innovation in the formulation of natural candles would be the incorporation of an organogel as a substitute of petrochemical paraffins.

AUTHOR CONTRIBUTIONS

All authors conceived and designed the study, and wrote the first draft of the manuscript, Marie Caroline Agogué carried out the research and analyzed the data. All authors contributed to and approved the final draft of the manuscript.

ACKNOWLEDGMENTS

The GEPEA laboratory would like to thank the company Denis & Fils and the ANRT for financing the PhD thesis for this work.

FUNDING INFORMATION

This study was funded by Denis & Fils Company (grant number: CIFRE 2017_00727).

ETHICS STATEMENT

This research falls outside of human or animal studies and institutional ethical approval was not required.

CONFLICT OF INTEREST

The authors declare no conflict of interest.

ORCID

Marie Caroline Agogué https://orcid.org/0000-0001-8981-6337

REFERENCES

Blake AI, Co ED, Marangoni AG. Structure and physical properties of plant wax crystal networks and their relationship to oil binding capacity. J Am Oil Chem Soc. 2014;91(6):885–903. https://doi.org/10.1007/s11746-014-2435-0

Canesi S. Table des fréquences de vibration caractéristiques en IR. Laboratoire de Méthodologies et Synthèse de Produits Naturels (LMSPN); 2020 Available from: http://lmspn.uqam.ca/fichiers/tablesir.pdf. [Accessed 13th January 2020].

Co ED, Marangoni AG. The formation of a 12-Hydroxystearic acid/vegetable oil Organogel under shear and thermal fields. J Am Oil Chem Soc. 2013;90(4):529–44. https://doi.org/10.1007/s11746-012-2196-6

Hwang H-S, Sanghoon K, Mukti S, Winkler-Moser JK, Liu SX. Organogel formation of soybean oil with waxes. J Am Oil Chem Soc. 2012;89:639–47. https://doi.org/10.1007/s11746-011-1953-2

Hwang H-S, Singh M, Bakota EL, Winkler-Moser JK, Kim S, Liu SX. Margarine from Organogels of plant wax and soybean oil. J Am Oil Chem Soc. 2013;90(11):1705–12.

INSA Rouen. Spectroscopie Infra Rouge - Tables détaillées des nombres d'onde; 2020. Available from: https://moodle.insa-rouen.fr/pluginfile.php/17255/mod_resource/content/0/tablesIR_detaillee.pdf.

Iwanaga K, Sumizawa T, Miyazaki M, Kakemi M. Characterization of organogel as a novel oral controlled release formulation for lipophilic compounds. Int J Pharm. 2010;388:123–8. https://doi.org/10.1016/j.ijpharm.2009.12.045

Jana S. Crystallization behavior of waxes. Utah State University - All Graduate Theses and Dissertations; 2016.

Kirilov P, Le Cong AK, Denis A, Rabehi H, Rum S, Villa C, et al. Organogels for cosmetic and dermo-cosmetic applications - classification, preparation and characterization of organogel formulations—part 1. Household Personal Care Today. 2015;10(3):15–9.

Kraus RS. Encyclopédie de sécurité et de santé au travail. 3rd ed. France: Bureau International du Travail. Industries Chimiques et Parachimiques; 2018.

Loisel C, Keller G, Lecq G, Bourgaux C, Ollivon M. Phase transitions and polymorphism of cocoa butter. J Am Oil Chem Soc. 1998; 75(4):425–39. https://doi.org/10.1007/s11746-998-0245-y

Merck. IR Spectrum Table by Frequency Range**. Available from: https://www.sigmaaldrich.com/technical-documents/articles/biology/ir-spectrum-table.html. [Accessed 21st November 2019].

Patel AR. Alternative routes to oil structuring. Germany: Springer; 2015. https://doi.org/10.1007/978-3-319-19138-6

Raemy A, Lambelet A. Thermal behaviour of foods. Thermochim Acta. 1991;193:417–39.

Rezaei K, Wang T, Johnson LA. Combustion characteristics of candles made from hydrogenated soybean oil. J Am Oil Chem Soc. 2002;79:803–8. https://doi.org/10.1007/s11746-002-0562-y

Rogers MA, Marangoni AG. Non-isothermal nucleation and crystallization of 12-Hydroxystearic acid in vegetable oils. Cryst Growth Des. 2008;8(12):4596–601. https://doi.org/10.1021/cg8008927

Rogers MA, Marangoni AG. Solvent-modulated nucleation and crystallization kinetics of 12-Hydroxystearic acid: a nonisothermal approach. Langmuir. 2009;25(15):8556–66. https://doi.org/10.1021/la8035665

Wang L, Wang T. Chemical modification of partially hydrogenated vegetable oil to improve its functional properties for candles. J Am Oil Chem Soc. 2007;84(12):1149–59. https://doi.org/10.1007/s11746-007-1147-0

Wauquier J-P. Raffinage du pétrole (Le). Tome 1. Pétrole brut. Produits pétroliers. Schémas de fabrication. Paris: TECHNIP; 1998.

Wu S, Gao J, Emge TJ, Rogers MA. Solvent-induced polymorphic nanoscale transitions for 12-Hydroxyoctadecanoic acid molecular gels. Cryst Growth Des. 2013;13(3):1360–6. https://doi.org/10.1021/cg400124e

How to cite this article: Agogué MC, Loisel C, Gonçalves O, Legrand J, Saint-Jalmes S, Arhaliass A. Multi-scale study of the structuration of candle blends with a high content of vegetable fats to replace paraffins: Effect of 12-hydroxystearic acid content. J Am Oil Chem Soc. 2022;99(12):1137–50. https://doi.org/10.1002/aocs.12625